KEK--91-12

JP9207092

KEK Report 91-12
January 1992
A

Quadrupole Modes in Linearized Beam-Beam Interaction in e^+e^- Colliding Rings

S. MATSUMOTO and K. HIRATA

NATIONAL LABORATORY FOR
HIGH ENERGY PHYSICS

© National Laboratory for High Energy Physics, 1992

KEK Reports are available from:

Technical Information & Library
National Laboratory for High Energy Physics
1-1 Oho, Tsukuba-shi
Ibaraki-ken, 305
JAPAN

Phone: 0298-64-1171
Telex: 3652-534 (Domestic)
(0)3652-534 (International)
Fax: 0298-64-4604
Cable: KEKOHO

Quadrupole Modes in Linearized Beam-Beam Interaction in e^+e^- Colliding Rings

Shuji MATSUMOTO and Kohji HIRATA,
KEK, National Laboratory for High Energy Physics,
Tsukuba, Ibaraki 305, Japan

Abstract

The dynamic-beta model is extended, incorporating the synchrotron radiation effects. The model yields dynamic-emittance effect. The steady-state envelope matrix is explicitly obtained. Both equal-beam and flip-flop solutions are found. The stability of the steady-state solutions are investigated by numerical calculations. The model illustrates some characteristic features of the beam-beam interaction at e^+e^- colliding rings in spite of containing some qualitatively unrealistic points.

Contents

1 Introduction

The dynamic-beta model[1] is the simplest model for the beam-beam effect on the coherent quadrupole motions in colliding storage rings. It gives the equilibrium transverse beam sizes of colliding beams under an assumption that the beam emittance is unaffected by the beam-beam interaction. The most significant ingredient of the model is that the beam-beam force is linearized. The beam-beam interaction can be simply regarded as an additional linear insertion at an interaction point(IP). This reduces greatly the complexity of the beam-beam problem because we can still work in a linear mapping theory if the other nonlinearity of the ring is negligible. This is just a prototype model. It gives a qualitative explanation for the luminosity perturbation due to the beam-beam interaction or the appearance of the flip-flop phenomenon[2]. In fact, they are found in real machines.

Apart from the linearization of the force, the dynamic-beta model has two shortcomings. One is that it assumes that the emittance is not affected by the beam-beam interaction. It is not so[3]. The other is that it treats merely the static aspect of the beam-beam problem. We, thus, have to make a small but essential modification on the model: we include the radiation effect explicitly and study the stability of the equilibrium solutions.

Furman, Ng and Chao (FNC) have presented a model similar to ours[4]. The difference lies in the treatment of the radiation. We employ the "symmetric radiation" whereas they employed the "asymmetric radiation". In the latter treatment, one assume that the

integrated effect of the diffusion over one turn has component only in the momentum direction in phase space. This seems somewhat unnatural. It seems quite difficult to design such a ring. Some of our results might be different from the ones of FNC model.

In the next section, we construct our model. The equilibrium solutions will be given in section 3. Investigation in the dynamical property of the solution by numerical calculations will be given in section 4. Section 5 is devoted to discussions.

2 The Model

Let us consider an e^+e^- storage ring. We will construct the model for the simplest case. The ring has only one IP. Each beam consists of a single bunch. Each bunch may contain different number of particles (N) and have different energy, but their ratio (N/γ) is the same. Here γ is the relativistic factor of the beam. The nominal betatron tune ν is common to both beams.

We will consider the ring in which the *nonlinearity* is negligible. And the beam-beam interaction is linearized with respect to the transverse coordinates of a particle. Thus we can work in a linear mapping theory. But *the whole dynamics is still nonlinear* because the beam-beam focal length for an electron depends on the positron transverse beam size (at the IP), and vice versa.

Now we will introduce the canonical variables X and P for the betatron motions. We define

$$X = \frac{x}{\sqrt{\beta}}, \quad P = \sqrt{\beta}x', \tag{1}$$

where x, x' are the betatron displacement and its slope respectively and β, common to the both beams, is the *nominal* (unperturbed) betatron function at the IP. The free betatron motion, the betatron motion of a single particle in the limit of no radiation, is a simple harmonic oscillation.

To study the coherent quadrupole motions, it is convenient to introduce the envelope matrix M, whose components are the quadrupole moments:

$$M = \begin{pmatrix} \langle X^2 \rangle & \langle XP \rangle \\ \langle PX \rangle & \langle P^2 \rangle \end{pmatrix}. \tag{2}$$

where $\langle\ \rangle$ indicates the average over the particle distribution in a bunch. This matrix determines uniquely the particle distribution in the phase space since it is always Gaussian in our model. This matrix is the basic dynamical variable in our model.

Let us consider the beam motion without the beam-beam interaction. The both beams perform the *coherent* betatron motion with radiation which is represented turn by turn, by the mapping

$$M \mapsto U M U^t + \mathcal{D}, \tag{3}$$

where

$$U = \begin{pmatrix} \cos(2\pi\nu) & \sin(2\pi\nu) \\ -\sin(2\pi\nu) & \cos(2\pi\nu) \end{pmatrix}. \tag{4}$$

Here, $2\pi\nu$ is the betatron phase advance in one-turn motion, U^t is the transposed of U and $\mathcal{D}$ is the integrated effect of radiation diffusion over one turn. And we write λ as

$$\lambda = \exp(-2\delta), \quad \left(\delta = \frac{1}{T_\beta}\right). \tag{5}$$

where T_β is the betatron damping time (measured in the unit of revolution time). Note that δ and $\mathcal{D}$ are determined by the lattice of the arc and can be represented by the radiation integrals[5]. We employ the symmetric radiation[3]:

$$\mathcal{D} = DI, \tag{6}$$

where I is the unit matrix[1].

The *fixed point* M_∞ of the mapping,

$$M_\infty = \lambda U M_\infty U^t + DI, \tag{7}$$

corresponds to an equilibrium state and we find

$$M_\infty = \frac{D}{1-\lambda} I. \tag{8}$$

It is fair to define the beam emittance as $\sqrt{\det M}$ so that the natural (unperturbed) beam emittance ϵ is given by

$$\epsilon = \sqrt{\det M_\infty} = \frac{D}{1-\lambda}. \tag{9}$$

The mapping, eq.(3), can be written now as

$$M \mapsto \lambda U M U^t + (1-\lambda)\epsilon I. \tag{10}$$

Once both the beams begin to collide with each other, we have to introduce two envelope matrices M^+ and M^- for each of the e^+ and the e^- beam, respectively. We will observe them at the moments just before they collide. The one-turn mapping in Eq.(3) should be rewritten as[2]

$$M^\pm \mapsto \lambda U K^\pm M^\pm \left(K^\pm\right)^t U^t + (1-\lambda)\epsilon I, \tag{11}$$

where each of the matrices $K^\pm$ represents the beam-beam kick for the $e^\pm$ beam:

$$K^\pm = \begin{pmatrix} 1 & 0 \\ -4\pi\xi_\pm & 1 \end{pmatrix}. \tag{12}$$

Here, $\xi_\pm$ are the so-called the *physical* beam-beam parameters. Hereafter, we will concentrate in the round-beam case only. In this case,

[1]The physical reason that $\mathcal{D} \propto I$: the each energy loss by the radiation at s gives the contribution proportional to $(D, \alpha D + \beta D')$, where D is the dispersion function. It is brought to the IP with betatron oscillation. Because the betatron phase advance from s to the IP changes a lot as a function of s, the sum of the contribution from all s becomes symmetric in the normalized phase space[3].

[2]Note that in eq.(11), ϵ is the nominal emittance, because it is nothing but the radiation integrals without beam-beam collision in different forms.

$$\xi_{\pm} = \left(\frac{Nr_0}{2\pi\gamma}\right)\frac{\beta}{2\sigma_{\mp}^2}, \tag{13}$$

where $\sigma_{\pm}$ is the r.s.m. transverse beam distribution of the $e^{\pm}$ beam, and r_0 is the classical electron radius. Note that $\xi_+(\xi_-)$ will be determined by the transverse beam distribution of the $e^-(e^+)$ beam(the strong-strong picture).

It is convenient to normalize the envelope matrices by the natural emittance ϵ. In the followings, we refer $M^{\pm}$ as the normalized envelope matrices: $M^{\pm}/\epsilon \to M^{\pm}$. In terms of them, the emittance ϵ is removed from the formulas in (3) and (11). Furthermore their $(1,1)$ components are just the normalized beam sizes squared.

$$\left(M^{\pm}\right)_{11} = \frac{\langle x_{\pm}^2\rangle}{\epsilon\beta} = \frac{\sigma_{\pm}^2}{\sigma_0^2}. \tag{14}$$

where σ_0 is the nominal beam size at the IP. Dynamics of the quadrupoles is described as an iteration of the one-turn mapping:

$$M^{\pm} \mapsto \lambda U K^{\pm} M^{\pm} \left(K^{\pm}\right)^t U^t + (1-\lambda)\, I. \tag{15}$$

We will write the kicks $-4\pi\xi_{\pm}$ in $K^{\pm}$ as

$$-4\pi\xi_{\pm} = -\frac{4\pi\eta}{\left(M^{\mp}\right)_{11}}, \tag{16}$$

where

$$\eta = \left(\frac{Nr_0}{2\pi\gamma}\right)\frac{\beta}{2\sigma_0^2}, \tag{17}$$

is a constant with which we refer the beam current. We call it the *nominal beam-beam parameter*.

Our model is now established. If we give the three parameters: the nominal tune $\nu(\mathrm{mod}\ 0.5)$, the nominal beam-beam parameter η and the betatron damping time T_{β}, and also give certain initial $M_{(0)}^{\pm}$, the first one-turn mapping will be determined. And the following one-turn mappings will be given turn by turn.

3 Period-One Fixed Points

In this section, we will examine the period-one fixed points of the one-turn mapping (15) in detail.

3.1 $\lambda \neq 1$ case; The scaling law

A period-one fixed point $M_{\infty}^{\pm}$ satisfy

$$M_{\infty}^{\pm} = \lambda U K^{\pm} M_{\infty}^{\pm} \left(K^{\pm}\right)^t U^t + (1-\lambda)\, I. \tag{18}$$

We can easily solve it. In terms of the components

$$M_{\infty}^{\pm} = \begin{pmatrix} a^{\pm} & c^{\pm} \\ c^{\pm} & b^{\pm} \end{pmatrix}, \tag{19}$$

we get

$$a^{\pm} = \frac{1 + 2\left(\sin^2\mu - \cos^2\mu + 2k_{\pm}\sin\mu\cos\mu\right)\lambda + \lambda^2}{1 + 2\{1 - 2(\cos\mu - k_{\pm}\sin\mu)^2\}\lambda + \lambda^2}, \tag{20}$$

$$b^{\pm} = \frac{1 + 2\{\left(1 - 2k_{\pm}^2\right)\left(\sin^2\mu - \cos^2\mu\right) + 6k_{\pm}\sin\mu\cos\mu\}\lambda + \left(1 + 4k_{\pm}^2\right)\lambda^2}{1 + 2\{1 - 2(\cos\mu - k_{\pm}\sin\mu)^2\}\lambda + \lambda^2}, \tag{21}$$

$$c^{\pm} = 2k_{\pm}\frac{\left(\sin^2\mu - \cos^2\mu + 2k_{\pm}\sin\mu\cos\mu\right)\lambda + \lambda^2}{1 + 2\{1 - 2(\cos\mu - k_{\pm}\sin\mu)^2\}\lambda + \lambda^2}, \tag{22}$$

where $\mu = 2\pi\nu$ and $k_{\pm} = 2\pi\xi_{\pm}$. From Eq.(16),

$$k_{\pm} = \frac{2\pi\eta}{a^{\mp}} \equiv \frac{\rho}{a^{\mp}}. \tag{23}$$

Plugging the last equations into Eqs.(20), we obtain a set of equations for $a^{\pm}$. Each solution gives the normalized equilibrium beam size of each $e^{\pm}$ beam. Notice that once we know $a^{\pm}$, then the other components $b^{\pm}$ and $c^{\pm}$ are also known right away. The equations for $a^{\pm}$ can be written as

$$a^{\pm} = \frac{1 + \rho\alpha\left(\frac{\sin\mu}{\sin\bar{\mu}}\right)^2\left(\frac{1}{a^{\mp}}\right)}{1 + 2\rho\alpha\left(\frac{\sin\mu}{\sin\bar{\mu}}\right)^2\left(\frac{1}{a^{\mp}}\right) - \rho^2\left(\frac{\sin\mu}{\sin\bar{\mu}}\right)^2\left(\frac{1}{a^{\mp}}\right)^2}. \tag{24}$$

where

$$\sin^2\bar{\mu} = \frac{(1-\lambda)^2}{4\lambda} + \sin^2\mu. \tag{25}$$

The difference between μ and $\bar{\mu}$ will be prominent if

$$\mu^2 \sim \frac{(1-\lambda)^2}{4\lambda} \equiv \Delta^2 (\ll 1). \tag{26}$$

But our model is valid only for the case $\Delta \ll \sin\mu$, because we have neglected the term of order δ/μ at the starting point (3). At any rate, $\Delta \sim \mu$ implies $\mu \to +0$ or $\mu \to \pi - 0$ and we need not consider these cases seriously because, in these cases the system must be unstable due to half integer resonances. Thus we can conclude that the influence of the radiation damping upon M_{∞} is very small because *always* $\sin\mu \simeq \sin\mu$. This small effect can be easily estimated if we know the solution in the no-radiation limit. Suppose we already know the M_{∞} in the no-radiation limit($\sin\mu = \sin\mu$ case). Then the solutions in a $\lambda \neq 1$ case are obtainable by the simple replacements:

$$\rho \to \rho\left(\frac{\sin\mu}{\sin\bar{\mu}}\right), \tag{27}$$

$$\alpha \to \alpha\left(\frac{\sin\mu}{\sin\bar{\mu}}\right). \tag{28}$$

To this end, all we have to do is to solve Eqs.(24) in the $\lambda \to 1$ limit.

3.2 $\lambda \to 1$ case: No-radiation limit

In the $\lambda \to 1$ limit, each of $M_\infty^\pm$ has a simple form[3]

$$M_\infty^\pm \to \frac{1+k_\pm\alpha}{1+2k_\pm\alpha-k_\pm^2}\begin{pmatrix} 1 & k_\pm \\ k_\pm & 1+2k_\pm\alpha \end{pmatrix}, \tag{29}$$

where

$$\alpha = \cot\mu. \tag{30}$$

The equations for $a^\pm$ would be

$$a^\pm = \frac{1+\rho\alpha\left(\frac{1}{a^\mp}\right)}{1+2\rho\alpha\left(\frac{1}{a^\mp}\right)-\rho^2\left(\frac{1}{a^\mp}\right)^2}. \tag{31}$$

There are two types of solution:

1. The equal-beam solution: $a^+ = a^-$.
2. The flip-flop solution: $a^+ \neq a^-$.

The first type is

$$a^\pm = \left(\frac{\sigma_\pm}{\sigma_0}\right)^2 = \frac{1}{2}\left(1-2\rho\alpha+\sqrt{1+4\rho^2\left(1+\alpha^2\right)}\right). \tag{32}$$

Notice that this type of solution always exists for arbitrary μ and $\rho(=2\pi\eta)$. The nature of the second one is a little intricate. We obtain from Eqs.(31)

$$a^+ + a^- = \frac{(\rho-\alpha)(1+2\rho\alpha)\rho}{1+2\rho\alpha-\rho^2} \equiv s, \tag{33}$$

$$a^+a^- = \frac{(\rho-\alpha)\rho^3}{1+2\rho\alpha-\rho^2} \equiv p. \tag{34}$$

Therefore, $a^\pm$ are the real and positive solutions of the quadratic equation:

$$x^2 - sx + p = 0. \tag{35}$$

It is shown that the last equation has two real and positive solutions [3] when

$$(0<)\,\rho_0 \le \rho < \rho_1\left(=\alpha+\sqrt{\alpha^2+1}=\cot\frac{\mu}{2}\right), \tag{36}$$

where ρ_0 is the positive root of the cubic equation,

$$-4\left(\alpha^2+1\right)\rho^3+4\alpha\left(\alpha^2+1\right)\rho^2+\left(3+4\alpha^2\right)\rho+\alpha=0. \tag{37}$$

(If there are two positive roots, ρ_0 is the larger one.) The solutions $a^\pm = \frac{1}{2}\left(s\pm\sqrt{s^2-4p}\right)$ exist in a restricted area on (α,η) plane. At the lower limit $2\pi\eta=\rho_0$, the equal-beam and two flip-flop solutions coincide with one another. On the other hand, at the upper limit ρ_1, a^+ tends to infinity while a^- goes to unity. This means one beam blows up and the other remains as if it were not perturbed. We will call the case, $2\pi\eta=\rho_1$, the "flip-flop limit" in this paper. See Fig.1.

[3] We use the condition that not only $a^\pm$ but $b^\pm$ should be positive.

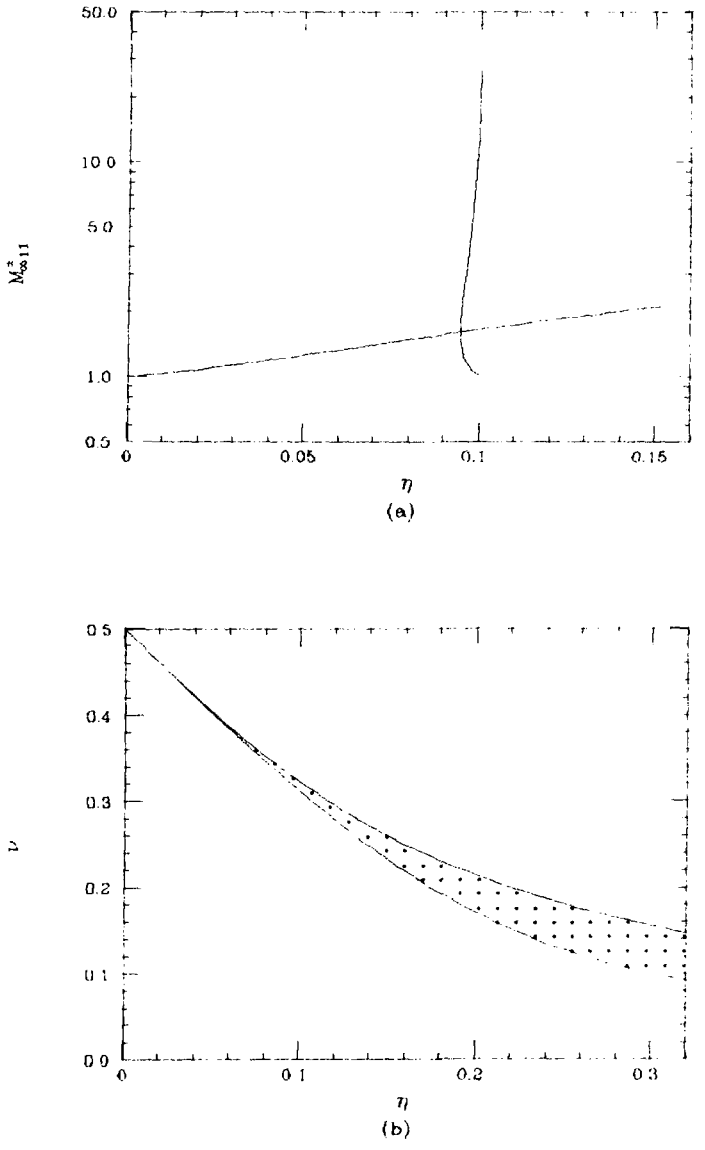

Figure 1: (a) Period one fixed points as a function of η. $\nu = 0.32$ and $\lambda \to 1$ limit. (b) Region where the flip-flop solution exists. $\lambda \to 1$ limit.

The equilibrium emittances $\bar{\epsilon}^{\pm}$ of the colliding beams are

$$\bar{\epsilon}^{\pm} = \epsilon\sqrt{\det M_{\infty}^{\pm}}, \tag{38}$$

and we obtain explicitly [3]

$$\epsilon^{\pm} = \epsilon\frac{1 + k_{\pm}\alpha}{\sqrt{1 + 2k_{\pm}\alpha - k_{\pm}^2}}. \tag{39}$$

Notice that $\epsilon^{\pm} \geq \epsilon$ always hold whatever $k_{\pm}$ are. This means the equilibrium emittances of both beams *always increase* once the both beams collide with each other.

4 Dynamics around the Period-One Fixed Points

The next issue is the stability of the period-one fixed points and the motion around them. We examine them by numerical calculations. All we have to do is to execute explicitly an iteration of the one-turn mapping (15) upon certain initial $M_{(0)}^{\pm}$ which might be slightly deviated from $M_{\infty}^{\pm}$. If a fixed point is stable, an initial perturbed state $M_{(0)}^{\pm}$ will converge to $M_{\infty}^{\pm}$. Otherwise some other dynamical state will appear.

4.1 About our numerical calculation

In our numerical calculation, we start with a state which is slightly perturbed from the equal-beam equilibrium state. We write[4]

$$\left(M_{(0)}^{\pm}\right)_{ij} = p_{(i,j)}^{\pm}\left(M_{\infty}\right)_{ij}, \quad (i,j = 1,2). \tag{40}$$

where M_{∞} is the matrix corresponds to an *equal beam* equilibrium state and all the coefficients $p_{(i,j)}^{\pm}$ are close to 1. In our calculation, we fixed $p^{\pm}$ as

$$p^{+} = \begin{pmatrix} 1.1 & 1.0 \\ 1.0 & 0.9 \end{pmatrix}, \quad p^{-} = \begin{pmatrix} 0.9 & 1.1 \\ 1.1 & 1.2 \end{pmatrix}. \tag{41}$$

The range of the tune is to be $0 < \nu < 0.5$. And we restrict the range of η as its maximum is to be $\frac{1}{2\tau}$, which is large enough for actual machines. We set $T_s = 100$ in the unit of revolution time. It is observed that 100 T_s turns is enough for convergence.

4.2 Stability of the period-one fixed points

To study the stability property of the fixed points, we first performed the numerical trackings for various η with a fixed tune. We found two distinct behaviors according to the tune ν: that is whether the tune is low, $\nu < 0.25$, or high, $\nu > 0.25$.

Fig.2 shows an example of the lower tune case. All the period-one fixed points seem to be stable when $\eta < 0.05$, whereas they are unstable otherwise. We found that whenever $\nu < 0.25$, the feature of the stability is similar to this example, i.e. at small η, the fixed points are stable whereas once η exceeds some critical value, a stochastic(both beam

[4]Repeated indeces do not mean to be summed in terms of them.

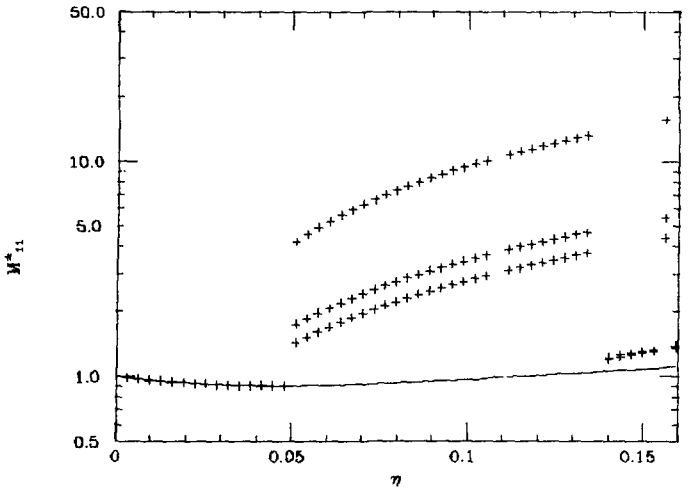

Figure 2: An example of lower tune case. $\nu = 0.15$ and $T_\beta = 100$. The solid line represents the period-one fixed points. For $\eta < 0.05$, the equal-beam state is stable. Period-3 states($\eta > 0.05$) and period-2 states(around $\eta \simeq 0.15$) are observed. It is found that $M^+ \simeq M^-$ always holds for multi-period states.

sizes change randomly turn by turn) or a multi-period state appears. In this example, the period-3 (and the period-2, when $\eta > 0.12$) state appears instead of the period-one. The appearance of such final states do depend on both the tune ν and the beam-beam parameter η. To see this, we will make tune survey in Section 4.3.

We can find some other features on the final states when we observe their normalized emittances $\sqrt{\det M^\pm}$. Fig.3 shows both $e^\pm$ beam emittances always increase definitely with increasing η except the critical points. One interesting feature is the $e^\pm$ beam emittances are almost the same, $\sqrt{\det M^+} \simeq \sqrt{\det M^-}$, in the multi-period or in the stochastic state, and are kept almost intact turn to turn. This means the beam distribution ellipses in the phase space keep their volume and rotate periodically(multi-period state) or randomly(stochastic state) turn to turn.

Fig.4 shows an example of the higher tune case. We can see that all the period-one fixed points are stable if they lie in the region below the flip-flop limit. In the region where both the equal-beam and the flip-flop states coexist, the system seems to choose the latter. Once η exceeds the flip-flop limit, the fixed points seem to be *truly unstable*, i.e. one beam will blow up while the other remains as if it were not perturbed. If $\nu > 0.25$, the stability property is just as same as the example in Fig.4, i.e. all the period-one fixed points are stable unless η exceeds the flip-flop limit.

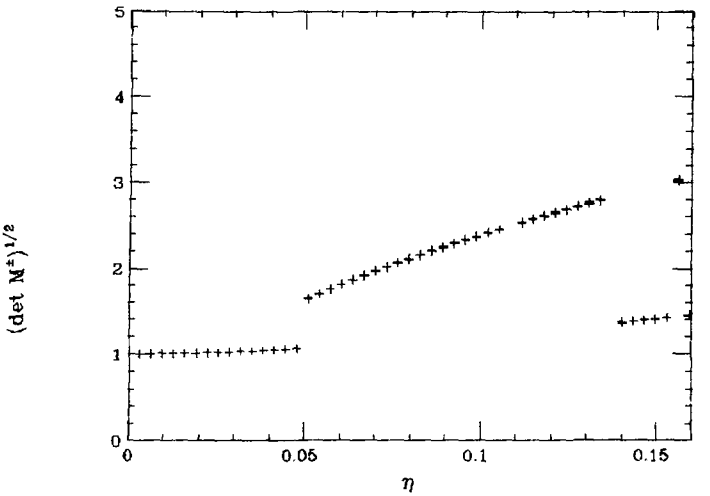

Figure 3: Observation of the normalized emittances $\sqrt{\det M^{\pm}}$ of the final states. $\nu = 0.15$ and $T_\beta = 100$. It is observed that both emittances are just same in an equal-beam state and almost same in a multi-period state. With increasing η, the emittances increase definitely. At the point where a period-3 state appears, the emittances jump up.

4.3 Tune survey

To see the way of appearance of the stochastic and the multi-period state, we observe $M_{11}^{\pm}$ for various ν under a constant beam-beam parameter, η. Fig.5 shows some examples and we can see a very interesting dynamical behavior. The region of the stochastic or the multi-period state is located just below $\nu = 0.25$. With increasing η, the area of the region gradually increases and more and more higher period states appear. We can see that more and more equal-beam states become unstable and some of them are push off into the multi-period state and others are fallen into the stochastic state.

The most interesting feature is the way of their appearance. A period-n state appears only in the region $\frac{1}{n+1} < 2\nu < \frac{1}{n}$. (For a very large η, however, we found some exceptions. See Fig.5(d). The period-two states exist in the region below $2\nu < \frac{1}{3}$.) Furthermore we can see the resonance-like structure, i.e. at the points $2\nu \to \frac{1}{2}, \frac{1}{3}, \frac{1}{4}, \ldots$, both beams blow up. An observation of the beam emittances shows this resonance-like structure more easily. See Fig.6.

The stochastic state appears only in a restricted region. It seems that they appear only in the *front* of the multi-period region, i.e. only in the small region in the lower tune side of the region of multi-period state.

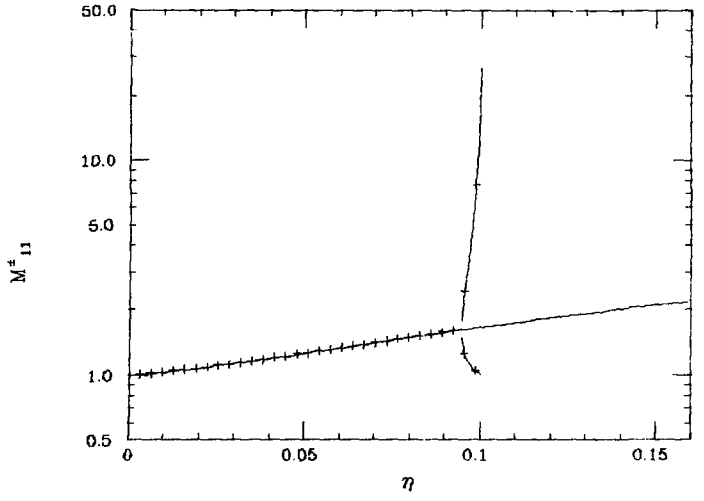

Figure 4: An example of the higher tune case. $\nu = 0.32$ and $T_\beta = 100$. The solid lines represent the period-one fixed points. The equal-beam states are stable until a flip-flop state appears. All the period-one fixed points are unstable when η exceeds the flip-flop limit. (All the final states fallen into the truly unstable state are suppressed in the figure.)

4.4 Effects of Radiation Damping

We found that radiation damping has a great influence on the stability of a final state in the lower tune case. With a larger damping time, some multi-period states seem to be basically unstable. See Fig.7. In the higher tune case, the effect of radiation damping is negligible as long as T_β is reasonably large.

We make a comment here. We found the scaling law of the period-one fixed points in Section 3.1. It connects the fixed point solutions with different damping time each other. However, the scaling law never tells us anything about the stability of the fixed points, since the scaling law is valid only among the static solutions.

4.5 Summary

The stability property of the period-one fixed points are summarized as follows. In the $\nu < 0.25$ case,

1. Stable for small enough η.
2. In the region where the flip-flop and the equal-beam states coexist, the former is stable while the later is not.
3. If η exceeds the flip-flop limit, the equal-beam states are unstable.

In the $\nu > 0.25$ case,

1. Same as 1 above.

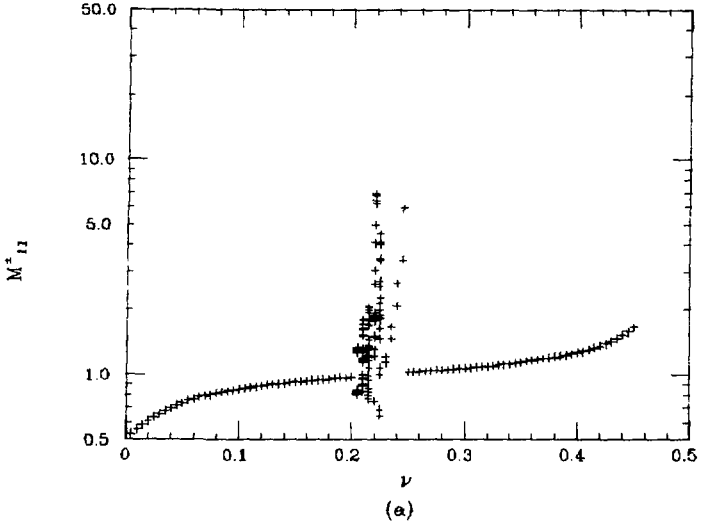
50.0
10.0
5.0
1.0
0.5
0
0.1
0.2
0.3
0.4
0.5
ν
M^2_{11}

(a)

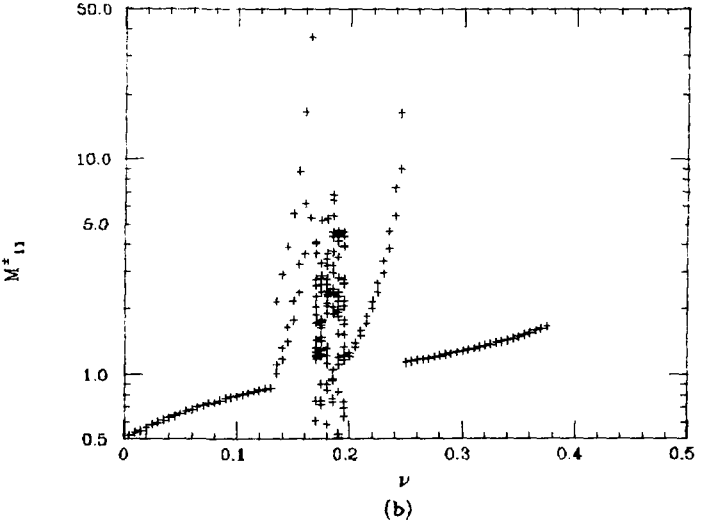
50.0
10.0
5.0
1.0
0.5
0
0.1
0.2
0.3
0.4
0.5
ν
M^2_{13}

(b)

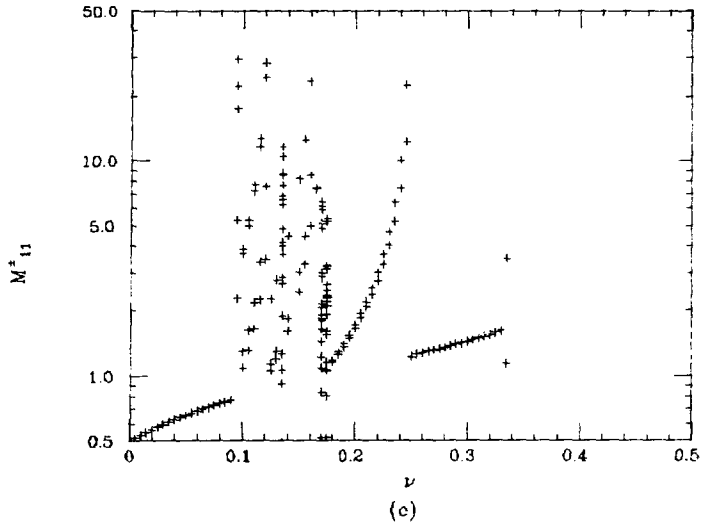

(c)

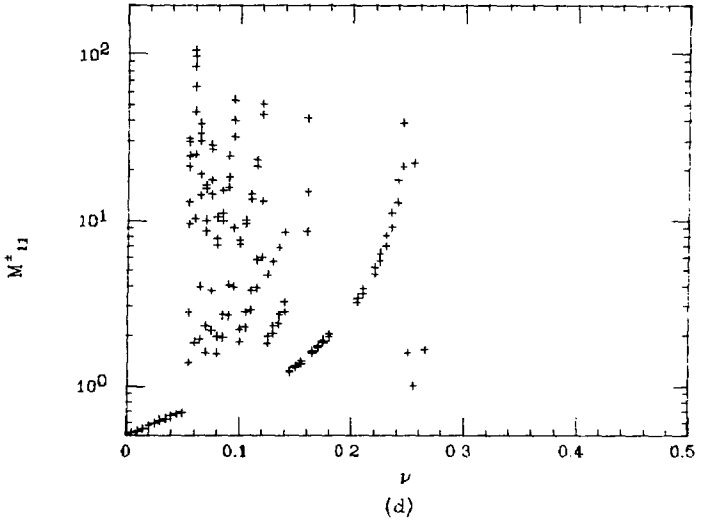

(d)

Figure 5: Results of our tune survey. (a) $\eta = 0.024$, (b) $\eta = 0.064$, (c) $\eta = 0.088$, (d) $\eta = 0.151$.

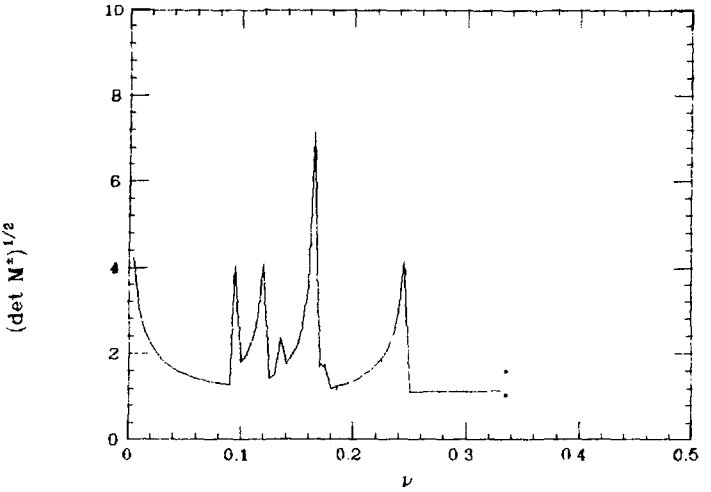

Figure 6: Observation of the normalized emittances $\sqrt{\det M^{\pm}}$ of the final states. $\eta = 0.088$. We can see the saw-tooth structure.

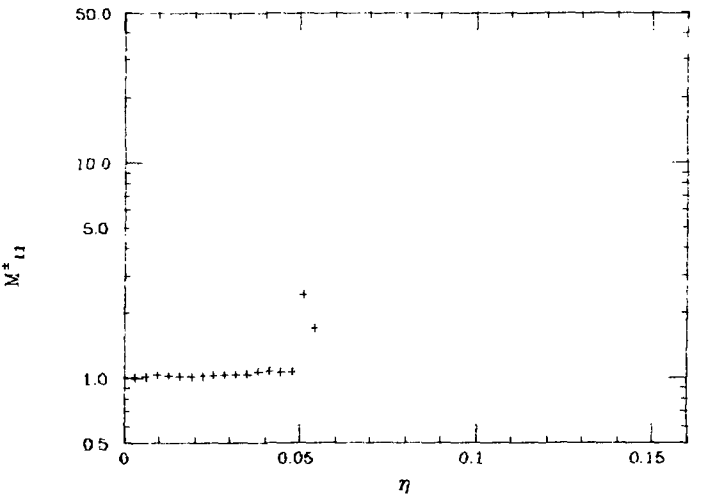

Figure 7: $T_\beta = 5000$ case. $\nu = 0.15$. All the calculations are stopped at 50000th turn. All the truly unstable final state are suppressed in the figure. All the multi-period states disappear. They seems to be basically unstable. Compare with Fig.2.

2. When η increases, the equal-beam state becomes unstable eventually. (The stochastic or the multi-period states appear instead.)

And we found the damping does have influence on the stability of multi-period states.

5 Discussions

We expect our model to explain various beam-beam effects. Among them, we are greatly interested in the effect on luminosity or the phenomenon of the beam-beam limit. We will discuss these respects based on the present model. We have constructed our model based on the symmetric radiation. We are also interested in how the present model gives the different results from the ones of FNC model which is based on the asymmetric radiation[3]. We will also pay attention in this respect.

5.1 Luminosity

At first we have to discuss our results from the point of view of luminosity. Luminosity is defined as

$$L = \frac{N^2 f}{4\pi\beta A^2}, \tag{42}$$

where $A^2 = \frac{\varepsilon}{2}\left(M_{11}^{+} + M_{11}^{-}\right)$ and f is the revolution frequency of a bunch. Generally speaking, for small η, the system will choose the equal-beam state as a final equilibrium state. It is easily seen by Eq.(32) and Eq.(42) that luminosity will be enhanced in a lower tune case($\nu < 0.25$), whereas it will be somewhat reduced in a higher tune case($\nu > 0.25$) compared with the nominal one. This effect is consistent with the dynamic-beta results[1], but quantitatively different due to the dynamic-emittance effect. When η exceeds a certain critical value, the system does not choose the equal-beam state anymore since it will be dynamically unstable. In fact, for example, we have seen that under a small perturbation from the equal-beam state, the system chooses the flip-flop state, the multi-periodic state or the stochastic state. At any rate, this is expected to yield a sudden reduction of luminosity. To see this, let us introduce the *effective* beam-beam parameter ξ which is defined as

$$\xi = \frac{2\xi_+\xi_-}{\xi_+ + \xi_-}, \tag{43}$$

then luminosity can be written in terms of it as

$$L = \frac{\gamma f}{r_0}\frac{1}{\beta} N\xi. \tag{44}$$

The effective beam-beam parameter ξ is defined turn by turn. However, we want to know its mean value. We introduce $\bar{\xi}$ as an average of ξ over many turns(say, over one damping time, T_β). Fig.8 shows the behavior of $\bar{\xi}$ in the case of $\nu = 0.15$ and 0.32. We start with $M_{(0)}^{\pm} = I$ (corresponding to the unperturbed equilibrium state). The sudden decrease of $\bar{\xi}$ comes from the appearance of a period-3 state in both cases, and this yields the reduction of luminosity. We call this phenomenon as the ξ-crash.

Here we find a new feature: the appearance of the final state seems to depend on the initial distributions $M_{(0)}^{\pm}$. The ξ-crash in $\nu = 0.32$ case in Fig.8 is due to the appearance

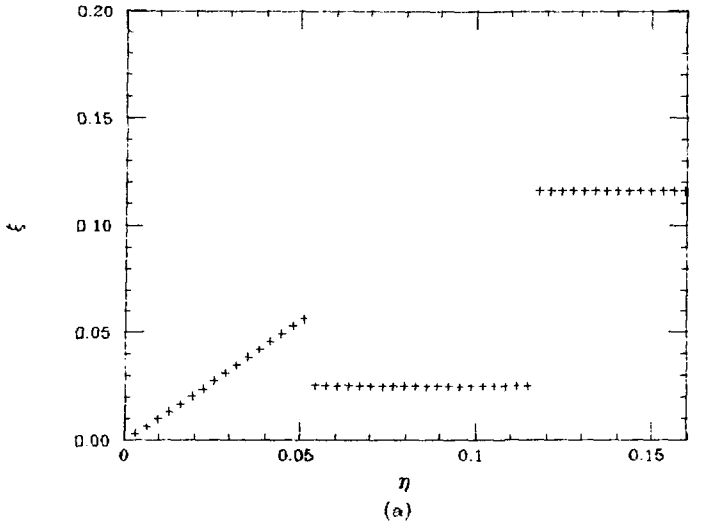

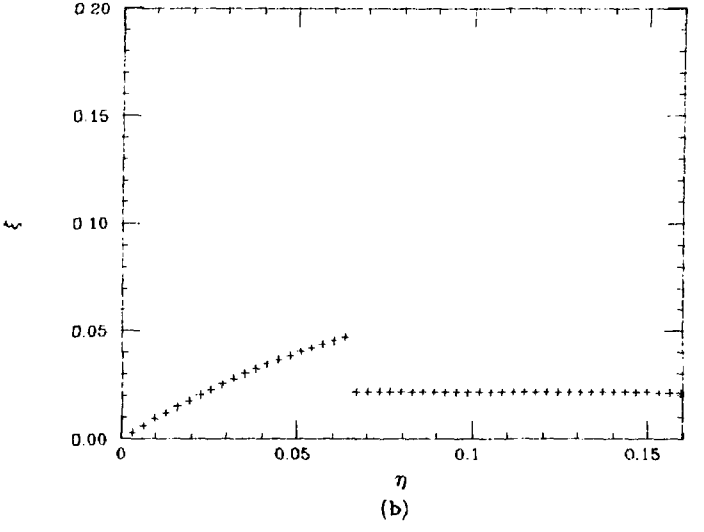

Figure 8: $\bar{\xi}$ in the case (a) $\nu = 0.15$ and (b) $\nu = 0.32$. $T_\beta = 100$ and $M^{\pm}_{(0)} = I$. In (a), there appear peroid-2 states for $\eta > 0.12$ and they give a rather large $\bar{\xi}$ value. We need not to consider it so seriously since the appearance of them depends on the inital distributions.

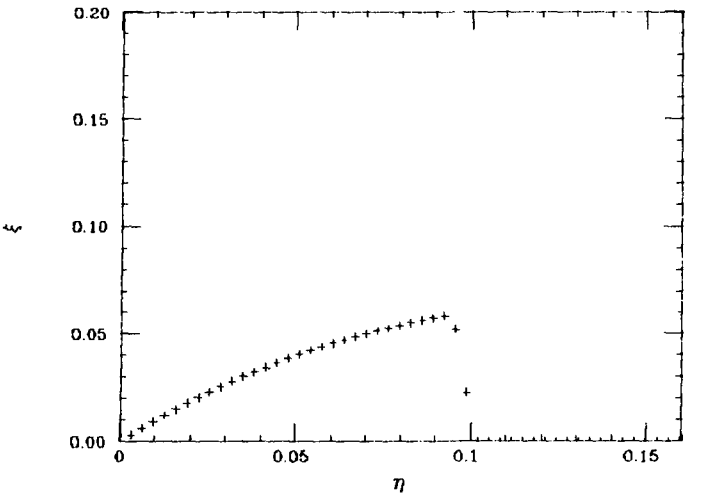

Figure 9: Dependence of ξ-crash behavior on the initial distributions $M^{\pm}_{(0)}$. We start with $M^{\pm}_{(0)} = pM_{\infty}$ in (40). $\nu = 0.32$, $T_{\beta} = 100$. Compare with Fig.8(b).

of a period-3 state. However such period-3 states never appear when we start with a state which is slightly perturbed from the equal-beam state, $M^{\pm}_{(0)} \sim M_{\infty}$, as we have seen(Fig.4). Fig.9 shows the effective ξ in this case. The difference obviously comes from the difference in the initial beam distributions. Generally speaking, the initial distributions $M^{\pm}_{(0)}$ are also responsible for what kind of state will appear as a final state. We will discuss this point in Section 5.4.

5.2 Beam-beam limit

We will call the point at which the ξ-crash occurs as the beam-beam-limit. When η comes near to this limit, the system falls into another state different from the equal-beam state and the luminosity will be reduced or the beam will be lost. We will see here the tune dependence of the beam-beam limit.

Again, we will start with $M^{\pm}_{(0)} = I$. See Fig.10. The beam-beam limit does depend on the tune. For the reasonable tune value, the beam-beam limits are around $\eta \sim 0.07$, which may be consistent with the observations in actual machines. The limit is mainly due to the appearance of the multi-period(or the stochastic) state if we choose $M^{\pm}_{(0)} = I$. However, this is inconsistent with various simulation results [6,7,8,9]. And it is also different from the result of the Gaussian model, in which the ξ-crash always attributes to the appearance of a flip-flop state[6]. The appearance of the multi-period states or the stochastic state seems to be the defect of the present model. However, when $\nu > 0.25$ and we start with a state which is slightly perturbed from the equal-beam state, $M^{\pm}_{(0)} \sim M_{\infty}$, the beam-beam limit always attributes to the appearance of a flip-flop state. An example was already

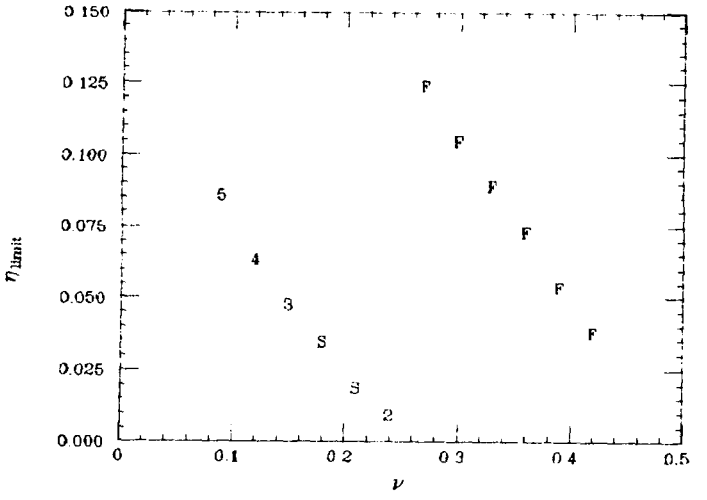

Figure 10: The tune dependence of the beam-beam limit. The limit attributes to the appearance of the various final states. F:flip-flop, S:stochastic, 2:period-2, 3:period-3, etc. $T_\beta = 100$ and $M^{\pm}_{(0)} = I$. (For $0.31 < \eta < 0.33$, there is a special and somewhat exceptional region where the stochastic state or the period-3 state are found. There, the ξ-crash occurs around $\eta \sim 0.05$ due to the appearance of these states.)

given in Fig.9.

The value of the beam-beam limit depends on not only the tune but the initial distributions of both beams, since the appearance of the final states depend on the initial distributions. However, its dependence on the initial distributions does not seem to be so clear as its dependence on the tune. The value of the beam-beam limit does not seem to be so changed by the initial distributions.

5.3 Difference between FNC model

Furman, Ng and Chao[1] studied a similar model to ours, but they employed the asymmetric radiation. To see the difference between our model and theirs, we observed the luminosity enhancement factor, $F = \xi/\eta$. See Fig.11. The initial condition is $M^{\pm}_{(0)} = I$. The sudden decrease of the enhancement factor comes from the appearance of a stochastic state(FNC) whereas a periodic-3 state(ours). The beam-beam limit value given in FNC model is a little smaller than ours. And the enhancement factor in FNC model seems to be too large(almost 1.4 at maximum even for small η) compared with the experiences of operating actual machines. In $\nu < 0.25$ case, the two models give the different results as shown by this example, but in $\nu > 0.25$ case, the difference is very small.

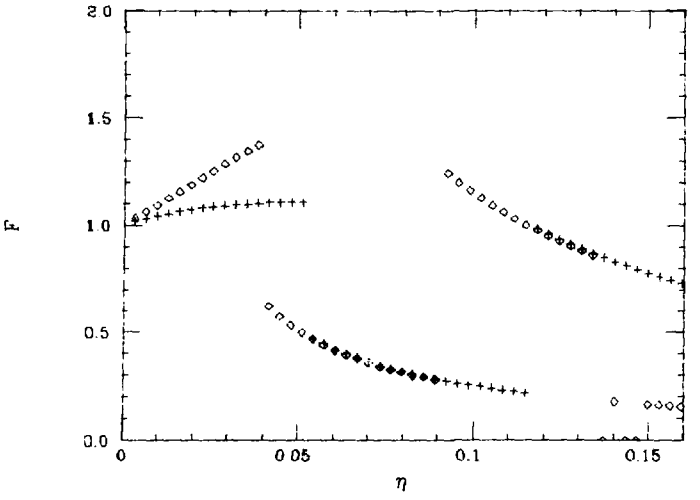

Figure 11: Difference between FNC model($\diamond$) and the present model(+). Observation of the luminosity enhancement factor, $F = \xi/\eta$. $\nu = 0.15$. $T_\beta = 100$. $M^{\pm}_{(0)} = I$.

5.4 Dependence on the initial conditions

Since we have already seen there is no uniqueness of the equilibrium state for a given ν and η, it is interesting to see how the final states depend on the initial distributions.

We need six parameters to identify the initial distribution: M_{11}, M_{12}, M_{22} for both beams. Let us confine ourselves to more restricted cases. Let us employ the initial condition as follows:

$$M^{+}_{11} = 1, M^{+}_{12} = 0, M^{+}_{22} = 1,$$
$$M^{-}_{11} = Q, M^{-}_{12} = 0, M^{-}_{22} = 1/Q. \tag{4.5}$$

That is, the e^- beam is mismatched to the lattice but has the correct natural emittance. In Fig.12, the final state values of $M^{\pm}_{11}$ are shown as a function of Q.

This restricted study shows us how a final state depends on the initial distributions $M^{\pm}_{(0)}$ in a complex way. This is another defect of the present model and we consider that it is due to the linearization of the beam-beam force. We have to pay attention to choosing the initial distributions.

6 Conclusion

We have studied the dynamics of the envelope matrix under the influence of the linearized beam-beam interaction and the radiation effects. Our model incorporates both the dynamic-beta effect and the dynamic-emittance effect. We employed the symmetric

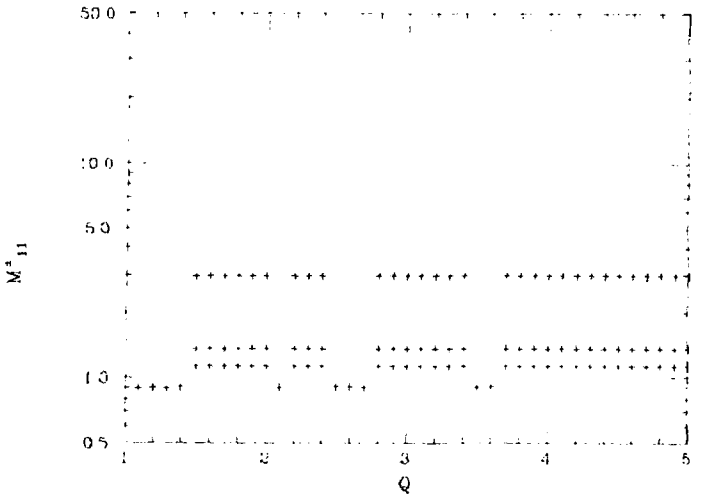

Figure 12: Q dependence of $M_{11}^{\pm}$. We start with the initial distributions given in (45). $\nu = 0.32$, $\eta = 0.04$. $T_d = 100$.

radiation. The most important ingredient is the linearization of the beam-beam force. And this enabled us to find the period-one fixed points in the explicit form and to work still in a linear mapping theory.

Our model has shown the beam-beam limit due to the flip-flop phenomenon or the multi-period (or the stochastic) motion. But the occurrence of latter seems to be the defect of the model: in more realistic simulation and the actual machines, such effects have never been observed so seriously. We found the final state depends on the initial distribution in a complex way. If it were true, the system is so sensitive to the initial conditions, so we cannot operate a machine.

Obviously, these defects come from the over-simplification of the beam-beam force. The linear force is too strong at the tail part. Once a beam blows up, the beam-beam effect should be reduced because it is effective only at the central part.

Apart from this point, our model seems to well illustrate the characteristic points of the beam-beam interaction. For example, it gives a reasonable value for the beam-beam limit. The simplicity is the most attractive point of the model. The present model is useful if we use it with careful consideration.

Acknowledgement The authors are grateful to Prof. Y. Kimura and Prof. T. Suzuki for their encouragement.

References

[1] B. Richter, Proc. Int. Symp. Electron and Positron Strage Rings. SACLAY. 1966. p I-1-1.

[2] A.W. Chao, Coherent Beam-beam Effects, SSCL-346 (1991).

[3] K. Hirata and F. Ruggiero, Treatment of Radiation in Electron Strage Rings, LEP Note 611 (1988); Particle Accel. **28**, 137 (1990).

[4] M.A. Furman, K.Y. Ng and A.W. Chao, A Symplectic Model of Coherent Beam-beam Quadrupole modes, SSC-174 (1988).

[5] R.H. Helm, M.J. Lee, P.L. Morton and M. Sands, IEEE Trans. Nucl.Sci.**NS-20**, 900 (1973).

[6] K. Hirata, Phys. Rev. Lett. **58**, 25 (1987);**58**, 1798(E) (1987); Phys. Rev. **D37**, 1307 (1988).

[7] E. Keil, Nucl. Instrum. Methods Phys. Res. **188**, 9 (1981)

[8] S. Myers, Nucl. Instrum. Methods Phys. Res. **211**, 263 (1983)

[9] A. Piwinski, in 11th Int. Conf. High Ener. Accel., Switzerland,1980, ed. W. S. Newman (Experimentia Supplementum, Vol. 40, Birkhauser, Basel, 1980) p.751